MITIGATION METHODS FOR SYSTEMATIC ERRORS IN USGS DEMs

Edward Russell, Computer Terrain Mapping, Inc.
Heidi Ochis, Computer Terrain Mapping, Inc.

INTRODUCTION

The USGS is in the process of acquiring Digital Elevation Models (DEMs) for all mapped 7.5 minute quadrangles (quads) in the United States and U.S. territories. This area comprises over 54000 quads, of which approximately 75% have had DEMs completed as of October 1997. This process began in the 1970s, and acquisition techniques have evolved over time.

The 7.5 minute DEMs consist of a UTM elevation grid sampled at a 30 meter spacing. The data are stored as "N-S" (in UTM space) oriented profiles (Figure 1).

The earlier techniques involved photogrammetric methods utilizing NHAP (National High Altitude Photography) and NAPP (National Aerial Photography Program) photos flown at approximately 40,000 feet and 20,000 feet nominal altitude respectively. Two photogrammetric methods were used: manual profiling (MP) and a stereocorrelation system referred to as the Gestalt Photomapper II (GPM or GPM2). Most DEMs produced prior to the early 1990s were acquired using one of these methods. Both techniques are characterized by distinctive systematic errors which are discussed below.
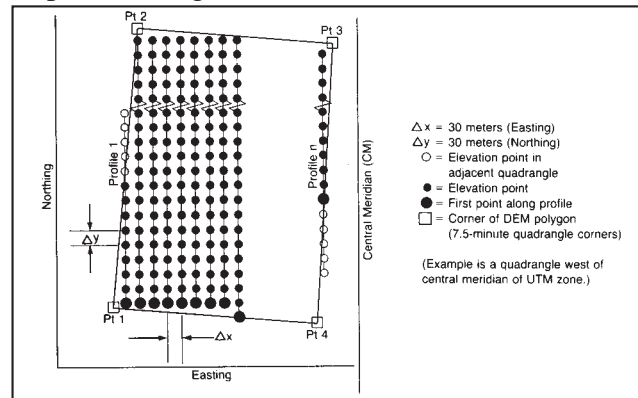
Figure 1. Structure of a 7.5 min. DEM, UTM meter grid (USGS, 1990).

Newer techniques involve estimating regularly spaced elevations using either scanned or photogrammetrically derived contours. These processes are often referred to as DLG2DEM or CTOG (contour to grid). Here, CTOG will refer to this class of contour to grid techniques and not to any specific software implementation.

The USGS has developed a three tiered level code which gives a rough classification of the DEM's quality. MP and GPM DEMs are designated as level 1. These files have maximum root-mean-square error (RMSE) values of between 7m and 15m. The CTOG DEMs are typically classified as level 2 with allowable RMSE values of one-half the map contour interval (typically 3m to 7m). Level 3 DEMs utilize CTOG methods, but may include hydrography, ridge line and elevation effects of major transportation features in their derivation. A maximum RMSE of one-third the contour interval is tolerated (USGS, 1990).

SYSTEMATIC ERRORS

Manual Profiling

Description

Figure 2 shows a shaded relief image of the Niwot, CO DEM, which was originally acquired via manual profiling (this DEM has been replaced with a newer CTOG DEM which will be

used in a later section for accuracy testing). This image displays the distinctive banding or striping which is the signature of this technique.

In the manual profiling process, an operator focuses a floating mark on the elevation surface of a stereomodel profile and collects elevation samples along the profile. These profiles are typically oriented in an E-W direction and the sample spacing along the profile is usually 30m. The traverse direction alternates from one profile to the next (e.g., left to right, then right to left) and the spacing between profiles varies with topographic relief, but is commonly 90m. The DEM is then interpolated from the sample points and reprocessed into the format described above (Russell, et al, 1995).
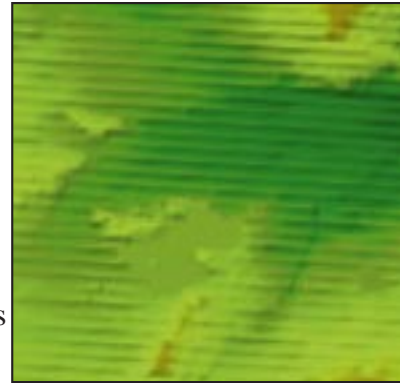

Figure 2. "Striping" problem in shaded relief image of Niwot, Colorado, 7.5 minute DEM.

The striping phenomena has been explained as a "lag" effect in the floating mark adjustment. So, for example, the floating mark "digs in" to a hill on one profile, then "rides high" off the hill on the next. There is some contradictory evidence to this explanation, however. Some profiles are persistently high or low, irrespective of the terrain. Also, striping often is worse in flat areas, which, by the "lag" explanation, should be least prone to errors. Most likely, the "lag time" explanation is only partially correct, and other factors such as operator error and machine miscalibration also contribute.

Figure 3. N-S elevation profile through the Niwot DEM.

Filtering method

The key to developing an effective filtering method is recognizing the essentially sinusoidal nature of the MP artifacts. Figure 3 shows a N-S elevation profile through the (manually profiled) Niwot DEM. This profile shows a distinctive sine wave pattern, particularly in the right-hand half. In this case, the wavelength of the anomalous sine wave pattern is about 250m.
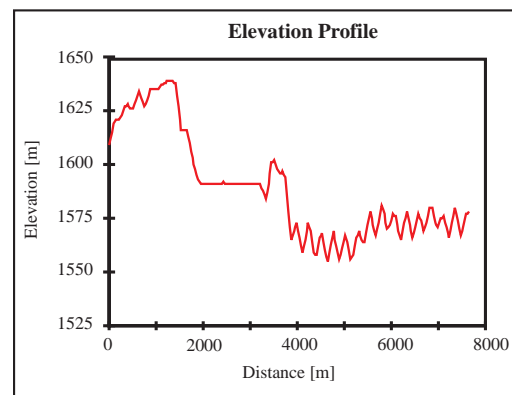
Using Fourier analysis, this spatial profile can be transformed into the frequency (wavelength) domain. Here, frequency refers to cycles/m, rather than cycles/s (hz) commonly used in time series analysis. Fourier analysis is useful for examining the contribution that each wavelength component makes to the spatial profile. One of the most common ways to display the results of the Fourier analysis is through a power spectrum graph or periodogram, which displays the relationship between spectral power (amplitude squared) and frequency or wavelength. Figure 4 shows the power
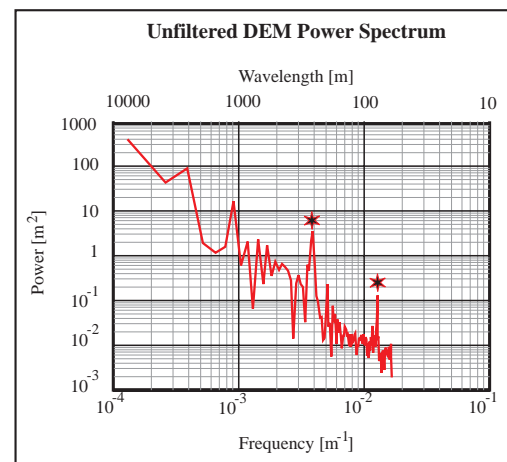

Figure 4. Power spectrum estimate for profile in figure 3. ✳ indicate regions with anomalously high amplitudes.

spectrum estimate for the profile shown in Figure 3. In this figure, two regions with anomalously high amplitudes are indicated by the stars. Figure 5 shows a series of power spectrum estimates stacked side-by-side to illustrate the geographic persistence of the anomalies.

The filtering technique described here affects only those portions of the power spectrum which display the amplitude anomalies. Figure 6 shows the filtered version of the power spectrum estimate shown in Figure 4. The regions (in frequency space) where the anomalies occur have been set to "background" levels. Figure 7 shows the resulting elevation
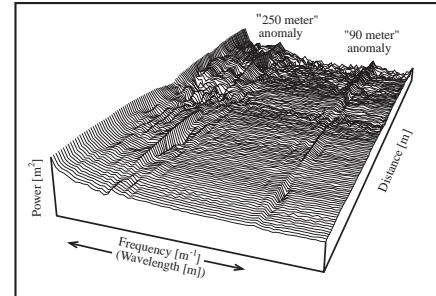

Figure 5. Perspective plot of power spectrum profiles for each N-S column of figure 2. The two amplitude anomalies are indicated.
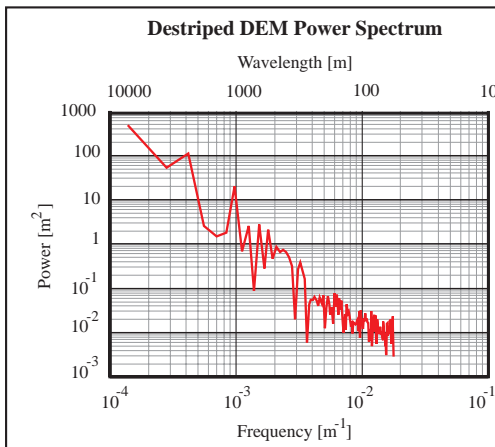

Figure 6. Power spectrum estimate for profile in figure 3 after destriping filter has been applied to DEM.
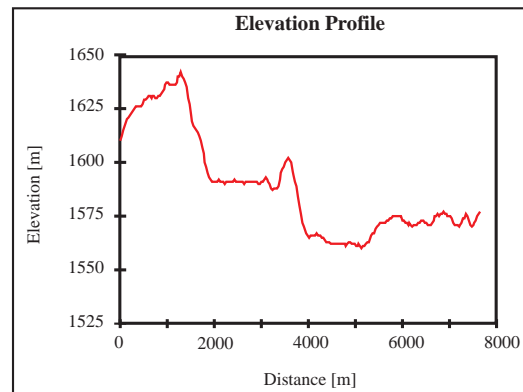

Figure 7. Resulting elevation profile when transformed back to the spatial domain after filtering.

profile when transformed back to the spatial domain after filtering. Because this method removes the "stripes" in the MP files, we refer to it as "destriping". Figures 8(a) and 8(b) show 3d views of the unfiltered and destriped DEMs.
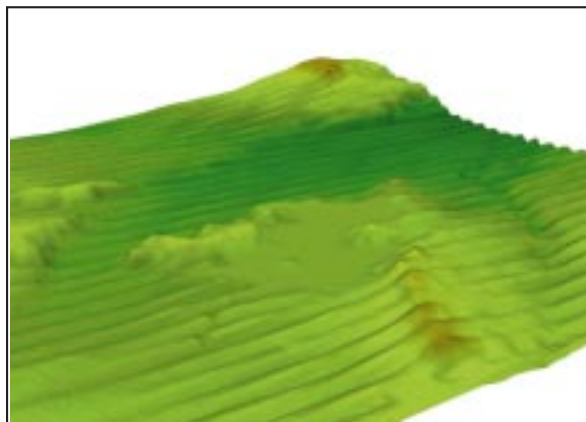

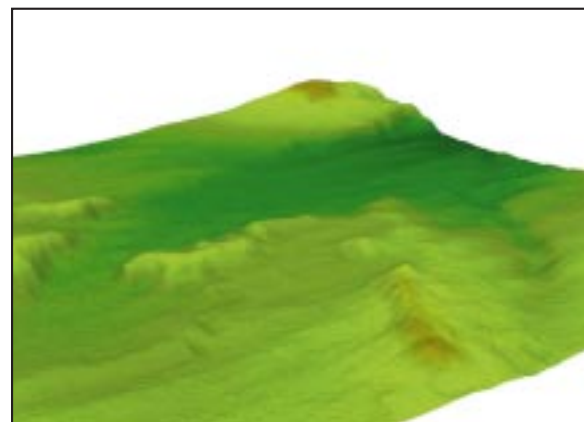Figure 8(a). 3d view of original MP Niwot, Colorado DEM.

Figure 8(b). 3d view Niwot, Colorado DEM after destriping filter has been applied.

Accuracy Assessment

As mentioned earlier, the original MP-derived Niwot file has been replaced by a newer CTOG-based file. One way to assess the effectiveness of the destriping technique is to compare the two DEMs. Figure 9 shows the results; the destriped DEM had a similar maximum error, while the RMSE was reduced by nearly 30%. Figure 10 shows a comparison of contours derived from (a) the unfiltered MP DEM, (b) the CTOG DEM, and (c) the destriped DEM.

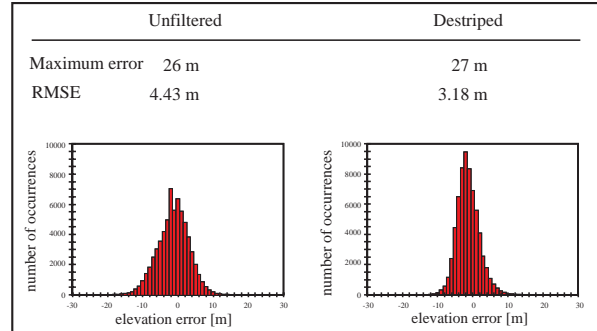|	Unfiltered	Destriped
Maximum error	26 m	27 m
RMSE	4.43 m	3.18 m

Figure 9. Accuracy assessment comparison between the unfiltered and destriped DEMs
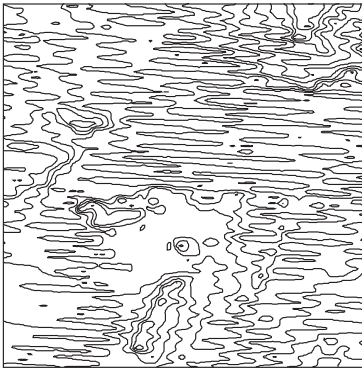

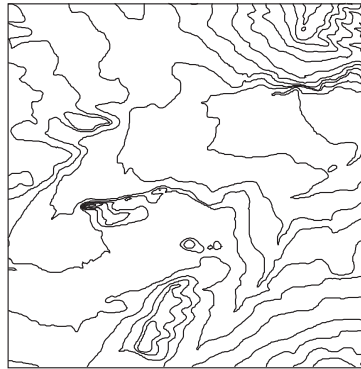Figure 10(a). Contours generated from unfiltered manually profiled DEM.

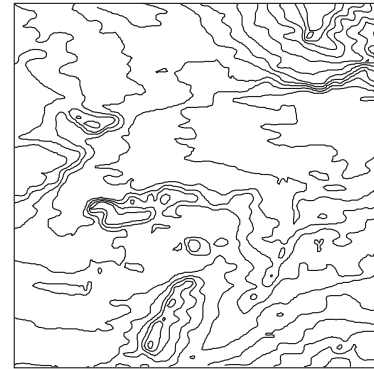Figure 10(b). Contours generated from CTOG DEM, "true" surface.

Figure 10(c). Contours generated from destriped DEM.

Gestalt Photomapper II

Description

Figure 11 shows a shaded relief image of the Louisville, CO DEM which was originally acquired via the GPM system (this DEM has been replaced with a newer CTOG DEM which is used in a later section for accuracy testing). This image displays the "quilted pattern" that characterizes many GPM DEMs: i.e., a noisy pattern within the quilt patches with frequent elevation discontinuities at the patch edges.

The Gestalt Photomapper II, an automated stereocorrelation system, is the other photogrammetric method for (level 1) DEM acquisition mentioned above. This system constructs the DEM in patches: small regions (9mm x 8mm) on the air photos in which elevations are measured by determining the parallax between correlated points in the airphoto stereopairs. The number of points used to interpolate gridded elevations varies with terrain conditions. These patches are then assembled to form the entire DEM and reprocessed into standard format (USGS, 1990).
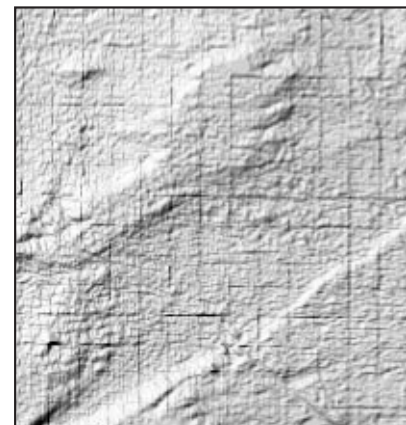

Figure 11. "Quilted pattern" in shaded relief image of a portion of the Louisville, Colorado 7.5 minute DEM. This pattern is characteristic of many GPM DEMs.

Filtering Method

Like the previously cited Niwot example, the Louisville quad also has two DEMs: one GPM and one CTOG. Figure 12 shows the cell-by-cell difference between the DEMs (GPM - CTOG) for a portion of the quad. The red areas are negative (GPM < CTOG), the blue areas are positive (GPM > CTOG) and the white areas have a difference of zero (GPM = CTOG). This illustrates the dual nature of the GPM anomalies: a noisy pattern within the patches, with prominent elevation discontinuities between patches. This dual error pattern also suggests two filtering techniques: one applied globally to deal with the noisy inner patch pattern, and one applied locally to deal with the patch edges.
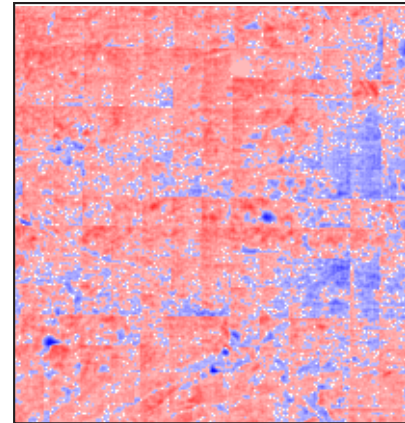

Figure 12. Cell-by-cell difference between DEMs (GPM-CTOG). Red areas are negative, blue areas are positive and white areas have the same elevation.

Global Filtering

It's common in signal processing to average time or space series values to improve signal-to-noise ratio. In fact, the average of n random samples from a distribution with mean μ and standard deviation σ, results in a sample mean that is a random variable with mean μ and standard deviation $\sigma/\sqrt{n}$. The "pseudo random" appearance of the inner patch noise makes averaging an obvious choice for noise reduction. (In practice, however, these assumptions may not hold. When averaging over some mxm window, it's likely that the true elevation will not be a constant μ throughout the window, but will vary, particularly as m gets large. In addition, the inner patch noise is probably not entirely random. Consequently, averaging will seldom produce an error decrease of the magnitude indicated above).

One downfall to averaging is the loss of resolvable detail; the larger the averaging window, the greater the loss of resolution. Also, as mentioned above, larger window sizes may result in lower accuracies. The goal is to choose a window size that combines accuracy improvement with minimal loss of detail. Table 1 shows the relationship between averaging window size and the computed standard deviation of the GPM - CTOG difference. Although the 5x5 window produces a slightly lower standard deviation, we've selected the 3x3 as a compromise between accuracy improvement and minimal resolution loss.

Table 1. Relationship between averaging window size and the computed standard deviation of the GPM-CTOG difference.

	unfiltered	3 x 3	5 x 5	7 x 7	9 x 9	11 x 11
RMSE [m]	3.28	2.89	2.82	2.96	3.23	3.57

Local filtering

For patch edges we've developed a special software tool that allows an operator to apply a "local" filter to an area of interest (AOI). Conceptually, this filter uses an nxn AOI window and a mxm averaging window (Figure 13).
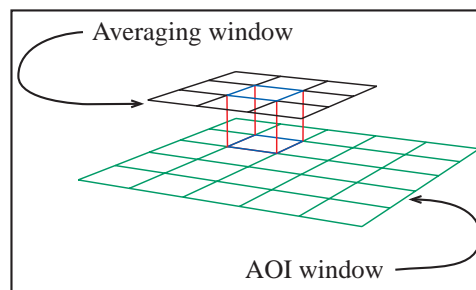

Figure 13. "Local" filter applied on an area of interest (AOI). The concept is based on a nxn AOI window and a mxm averaging window.

The operator chooses the location of the AOI window interactively by viewing an elevation tinted, hillside shaded image of the DEM. The averaging window visits every cell of the AOI window. The resulting elevation values within the AOI window are weighted according to their positions within the window (Figure 14). This weighting is defined by:

$$\zeta_{ij} = w_{ij}z_{ij} + (1 - w_{ij})\,\bar{z}_{ij}, \text{ where}$$

ζ_{ij} is the resulting (output) elevation value for row i, column j,

z_{ij} is the original elevation at (i,j),

$\bar{z}_{ij}$ is the average over the m x m window centered on cell (i,j),

w_{ij} is the "distance" (from AOI center) weighting function. Specifically,

$$w_{ij} = \max(\mathrm{abs}(i\text{-}ic), \mathrm{abs}(j\text{-}jc))/(n/2 + 1),$$

where (ic,jc) is the index of the center cell in the AOI and n is the AOI size in rows or columns (AOI is nxn window).

AOI window

$1 \times \bar{z}_{ij} + 0 \times z_{ij}$ $.75 \times \bar{z}_{ij} + .25 \times z_{ij}$

$.50 \times \bar{z}_{ij} + .50 \times z_{ij}$ $.25 \times \bar{z}_{ij} + .75 \times z_{ij}$

$z_{ij} = $ original elevation at (i,j)
$\bar{z}_{ij} = $ average over mxm window centered on cell (i,j)
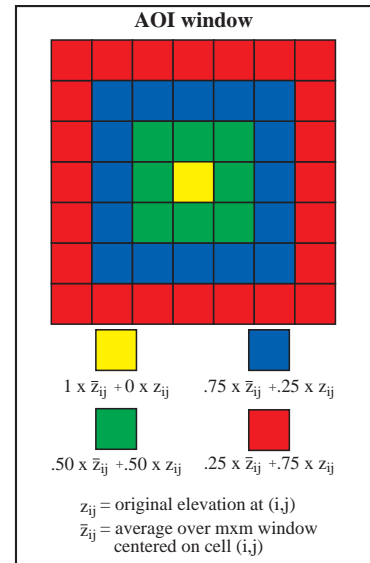
Figure 14. Resulting elevation values within a 7x7 AOI window are weighted according to their positions within the window.

The elevation color and hillside shading are adjusted "on the fly" based upon the new elevation values.

Two important factors provided motivation for this filter design:
1. The AOI window is utilized to allow the user to affect a multi-cell region with a single operation. Performing operations on a cell-by-cell basis tends to be slow and tedious.
2. The weighting scheme was designed to transition smoothly between filtered and unfiltered cells, avoiding a "footprint" of the AOI window.

In summary, an mxm mean is calculated for every cell within the AOI. The resultant elevation value at a cell is the weighted average of this mxm mean, centered at the cell, and the original elevation value at that cell. The weighting is dependent upon the distance of the cell from the AOI center. Figures 15(a) and (b) show a shaded relief image of the Louisville DEM before and after filtering.
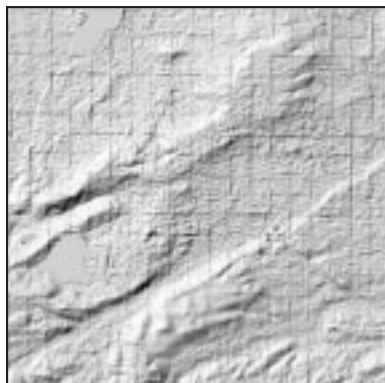

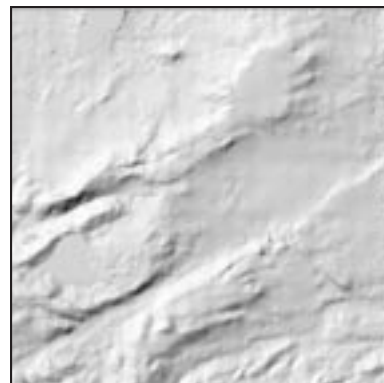Figure 15(a). Unfiltered GPM DEM.

Figure 15(b). Filtered GPM DEM.

Accuracy Assessment
As in the MP example, the accuracy is assessed by comparing the original GPM DEM to the newer CTOG version. Table 2 shows this comparison; maximum error was slightly reduced, while the RMSE was reduced by approximately 15%.

Table 2. Comparison of original GPM DEM and filtered DEM to the newer CTOG version.

	unfiltered	filtered
RMSE [m]	3.28	2.79
Max error [m]	24	22

Edge Matching

Description
Figure 16 shows a shaded relief image of the region where the Climax, Copper Mountain, Leadville North and Pando, CO quads join. The quad edges are readily apparent due to elevation discontinuities between adjacent DEMs. Edge matching problems between DEMs are quite common and are not restricted to level 1 files.

Figure 16. Shaded relief image of region where Climax, Copper Mountain, Leadville North and Pando, CO quads join.

Figure 17. Shaded relief image of region where Climax, Copper Mountain, Leadville North and Pando, CO quads join after the local filter has been applied.

Filtering Method
The local filter described in the GPM section is the filtering method of choice. Adjacent DEMs are tiled or mosaicked together, and the local filter is applied to the quad edge discontinuities. Figure 17 shows the shaded relief image of the same area after the filter has been applied.

SUMMARY

USGS level 1 7.5 minute DEMs are prone to characteristic systematic errors, depending upon the acquisition technique. The two filtering methods described in this paper produced measurable accuracy improvements in two sample USGS quads. In addition to accuracy improvements, the visual quality of the DEM as well as derived products (contours, slope, aspect, etc) is greater enhanced.

Edge-matching problems between adjacent DEMS are not limited to level 1 files. A method is described which mitigates these edge-matching problems.

REFERENCES

Russell, E., M. Kumler and H. Ochis, 1995. Identifying and removing systematic errors in USGS DEMs, *GIS in the Rockies Conference Proceedings*, Denver, CO (Sep 25-27, 1995).

USGS, 1990. Digital Elevation Models, Data Users Guide 5. Reston, VA: U.S. Geological Survey.